In-situ accelerated testing of bituminous mixtures

A.M. Hartman[1] — M.D. Gilchrist[1] (✉)
P.M.O. Owende[2] — S.M. Ward[2] — F. Clancy[3]

[1] *Mechanical Engineering Department*

University College Dublin, Belfield, Dublin 4, IRELAND

{Anton.Hartman; Michael.Gilchrist}@ucd.ie

[2] *Department of Agriculture and Food Engineering*

University College Dublin, Earlsfort Terrace, Dublin 2, IRELAND

{Philip.Owende; Shane.Ward}@ucd.ie

[3] *National Roads Authority*

Pottery Road, Dun Laoghaire, Co. Dublin, IRELAND

FClancy@nra.ie

ABSTRACT: *The in-service behaviour of a standard Irish Dense Base Coarse Macadam mixture (DBC) was evaluated by using the material to overlay a road section, which was based upon a weak pavement structure. The response of the layer under a fully laden dual axle truck was examined using a series of pressure cells and asphalt strain gauges that were embedded in the test section. The section was traversed repeatedly until a network of fatigue cracks was observed on the road surface. The transverse horizontal tensile strain was found to be the most critical parameter with respect to crack initiation. When based on in-situ measured strain data, the analytical model that was developed to predict pavement performance on the basis of fundamental laboratory test data, was found to underestimate the in-service fatigue life of the DBC mixture by a factor of 13.5. The underestimation may be attributed to factors that are not accounted for in the analytical models such as material healing, traffic wander and in-situ environmental conditions, which possibly lead to lower fatigue estimates.*

KEY WORDS: *accelerated loading test, asphalt strain, bituminous mixture, fatigue cracking*

1. Introduction

There are particular advantages that are uniquely associated with full-scale test facilities over simulated laboratory test programmes. The effects of size, manufacturing, environment, substructure and loading represent much more closely the on-site conditions than can be simulated directly with scaled models. However, full-scale test facilities, which are generally in outdoor ambient conditions, do not permit temperature and moisture to be controlled and consequently there are always inherent disparities relating laboratory and in-situ test data.

Recent research has focussed on the mechanical performance of standard Irish bituminous mixtures using simple laboratory uniaxial fatigue tests [HAR 00, HAR 01a] and simulation fatigue wheeltracking tests [HAR 01b]. This present paper describes a full-scale accelerated loading performance test on one of the investigated materials: a 20mm Dense Base Coarse Macadam [BS 93]. The performance test was done in conjunction with a related project, focussing on the influence of tyre inflation pressures on the degradation of peat based forest access roads [OWE 01]. Such forest roads generally have a weak pavement structure, which consists of surface dressed granular pavement layers ($\approx$ 0.5m deep) that overlay deep peat foundations. In general, peat (a soft biogenic deposit) provides a poor foundation for roads as it is frequently weak [O'MA 00] and compressible, particularly after prolonged dry periods [DAV 96].

Various pavement monitoring procedures exist, the most basic being the evaluation of structural integrity through monitoring of crack initiation and propagation, and permanent deformation on the pavement surface. Vertical and horizontal strains, vertical stresses and deflections are the physical parameters most frequently used in the related analysis [ULL 87]. In-situ material properties can be evaluated by measuring surface deflections with a Falling Weight Deflectometer (FWD), while internal stresses and strains can be monitored by use of appropriate transducers located at critical positions within the pavement structure. Pertinent environmental factors such as moisture level in the subgrade and pavement temperature are also monitored.

The focus of the present research was aimed at characterising and quantifying the in-situ mechanical performance of a standard Irish Dense Base Course Macadam (DBC) by measuring surface strains, crack growth and subgrade stress at incremental levels of fatigue cycles under controlled load conditions. Information pertaining to wheel loads, contact pressures, and road substructure were also monitored to facilitate the accurate assessment and diagnosis of section failure.

2. Selection and layout of test section

A section of a forest access road located between Knockananna and Kilcarney in County Wicklow (Ireland), was identified for the experiment. The section was chosen based on the following criteria:

- the site had to be well drained to prevent seasonal rainfall from causing premature pavement failure,
- the subgrade had to behave in as stable a manner as possible with seasonal changes and had to provide adequate support against surface deflections,
- the surface had to have the minimum amount of obvious defects to ensure original crack failure, and
- the section had to be reasonably level so as to minimise dynamic overloading effects.

A series of FWD surface deflection measurements (at 5m intervals) was made to assess subgrade conditions before the final 35m test section was selected. The measured deflections were very high (typically the maximum deflection, D_0 > 2000μm), and characteristic of the weak, shallow pavement structure and the peat subgrade conditions.

Figure 1 shows a schematic layout of the monitoring section, the dimensions of which are 3.3m (road width) by 35m (length of overlaid area). A central area in the outer wheelpath was selected for instrumentation with pavement transducers, the layout of which is shown in Figure 2. The initial FWD measurement positions, located in the outer wheel path were relocated after construction of the overlay and subsequent measurements were taken at the same positions. An extra FWD point was marked over the instrumented area to compare backcalculated and measured pavement responses. Crack monitoring grids were randomly spaced in the outer wheelpath over 15m along the section. A total of 19 grids were marked out to monitor cracking. Four permanent deformation cross section measurement positions were identified, two at both ends of the crack monitoring strip. The traffic counter was located at the end of the test section. The counter had to be placed as far away as possible from the crack monitoring and permanent deformation measurement positions since counter cables had to be machined into the overlay which could induce initial defects.

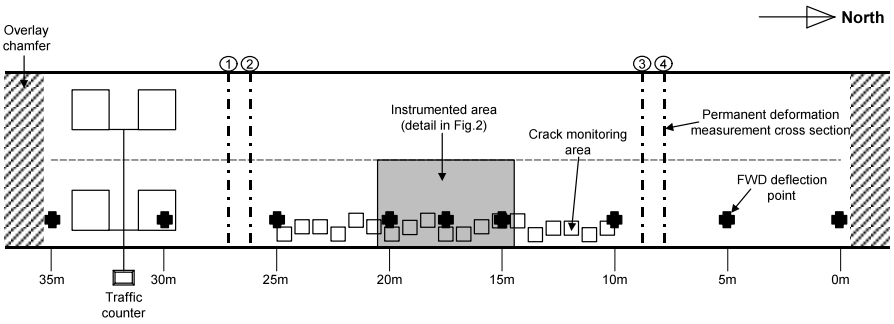

Figure 1. *Layout of the experimental road.*

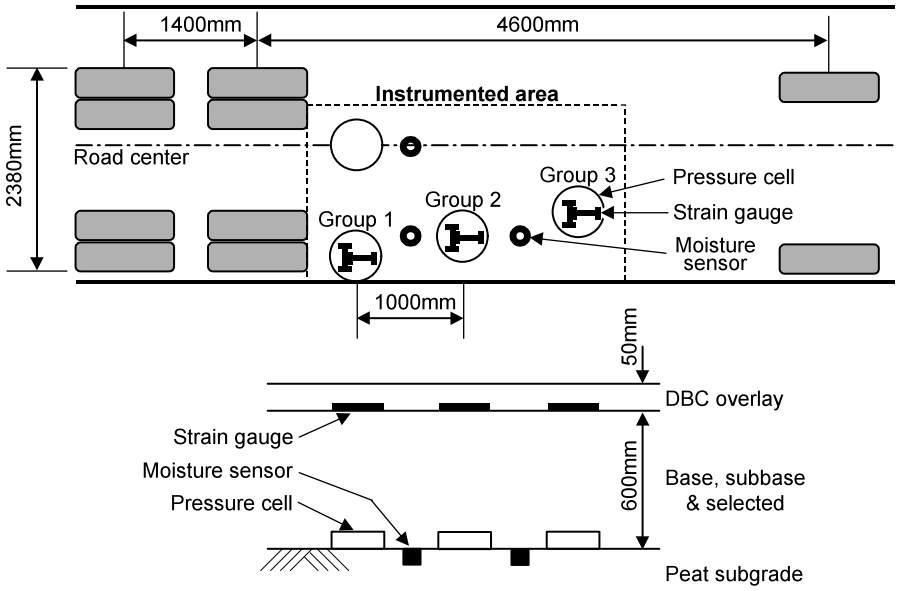

Figure 2: *Layout of sensors and transducers within instrumented area; superimposed axle spacing and track width of experimental truck (DBC = Dense Base Course overlay).*

3. Construction of test section

3.1. *In-situ material properties*

During excavation of the testpit to insert the pavement instrumentation, details of the in-situ pavement layers were noted and samples were taken for laboratory analysis and classification. The surfacing consisted of a thin bitumen seal that overlaid an 80mm thick crushed stone base, which itself was on top of a sandy subbase. At 600mm depth the peat subgrade was uncovered. The peat had a typical high moisture content (344% by wt.) that caused the subbase to soak up moisture (10.4% by wt.). The structural load carrying capacity of the base and subbase material was reasonable and California Bearing Ratio's (CBR) at in-situ densities of above a hundred were measured. The layers were all fairly sandy/silty, indicated by non-plasticity and low shrinkage values (< 3%). Care was taken not to segregate material from the different layers so that the same material could be used to reconstitute the pavement after installation of the sensors.

3.2. *Installation of pavement instrumentation*

To measure pavement response, asphalt strain gauges and soil pressure cells were installed at critical positions within the pavement structure. These positions were identified as being at the bottom of the asphalt overlay and on top of the subgrade. Additionally, moisture sensors and temperature probes were placed to monitor the in-situ temperature and moisture levels. Table 1 gives a summary of the types of gauges that were used, the number of gauges installed and their respective manufacture's details.

Table 1. *Summary of measurement instrumentation installed in the instrumented area of the experimental road section.*

Device	Number installed	Model	Manufacturer
Pressure cell	4	TP-101-S	RST Instruments
Strain gauge	6	PAST 2-AC	Dynatest
Moisture sensor	3	257	Campbell Scientific
Temperature probe	3	107	Campbell Scientific

The monitoring instrumentation (excluding the traffic counter) was installed in the testpit, 0.6m deep and 3 x 2m in area. The basic layout and position of the

different sensors are shown in Figure 2. The four pressure cells were laid on top of the peat subgrade. Three of the cells were staggered over the wheel path while the fourth was located in the centre of the road. Fine sand was used as bedding material to prevent large stones from causing localised pressure points on the sensitive surfaces of the cells. Soil moisture sensors, each fitted with a reference temperature probe, were inserted into the subgrade and covered with perforated plastic cups to prevent compaction damage. The excavated area was reconstituted with the original material using a hand operated vibratory compactor. In-situ densities were not verified but deflection measurements, discussed in section 6.1.2, indicated a weakening of the pavement structure at the testpit. The area was then sealed with a 10mm single seal.

The asphalt strain gauges were installed at the time of the overlay construction. The strain gauge application points were smoothed to remove sharp and large aggregates from under the transducer and the gauges were positioned in the longitudinal and transverse directions. Grooves were cut through the existing surfacing and the lead wires from the strain gauges inserted into the grooves. The grooves were then filled with fine aggregates to protect the wire from damage during construction and loading. Mixture fines were sieved over the gauges and hand compacted to fix them into position. After the gauges were properly located construction of the full width layer was resumed; this involved the use of plant compaction equipment. All the sensor cables were soldered to individual sockets in a terminal box that was located at the roadside.

3.3. *Construction and properties of asphalt overlay*

The total size of the overlaid area was approximately 120m^2; this required about 15 tonnes of mix to cover. Due to restrictive site access and subgrade conditions, the material had to be laid by hand. The area was sprayed with a tack coat after which the hot mixture was spread by wheelbarrow and rake. During the laying operation, loose mix was sampled to evaluate the mixture composition. Figure 3 shows the achieved aggregate grading. The bitumen content (4.3% by wt.) was purposely chosen towards the lower end of the design spectrum (4.7% ± 0.6%, [BS 93]) to obtain a fatigue prone mixture. The compaction temperature was monitored with a hand held probe at around 110°C. The long hauling time from Dublin (approximately 5h), the manual nature of the laying operation and the low air temperature (< 10°C) resulted in rapid cooling of the mixture and a low compaction temperature. This, combined with the light weight compaction plant (0.5 tonnes pedestrian roller) and the weak foundation support, resulted in poor densities being achieved (voids > 10%).

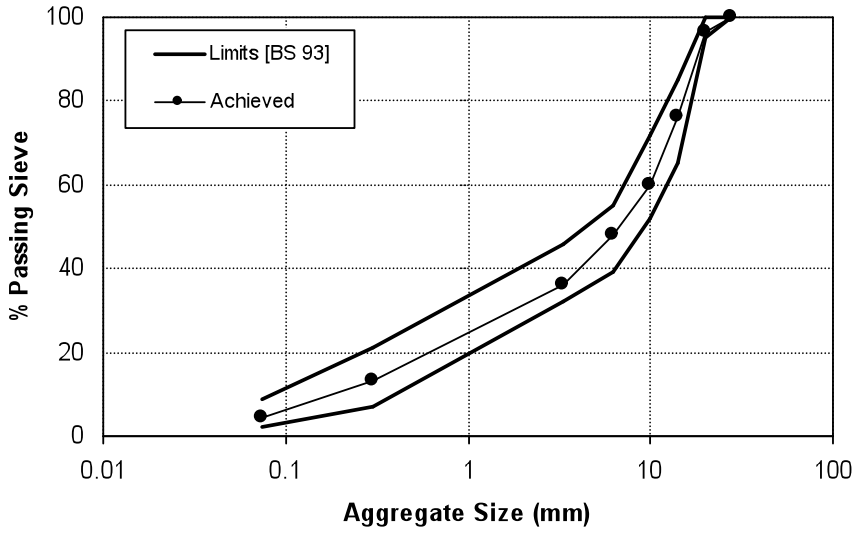

Figure 3. *Aggregate grading for the DBC mixture.*

Core specimens were machined from the section in order to determine the quality of the compaction effort and to measure the layer properties. Table 2 summarises the material properties that were measured from the cores. The very high void content measured, however, could also be related to the position from where the cores were machined: cores were machined at the beginning and end of the test section, away from the crack and permanent deformation monitoring areas. These positions corresponded to material taken from the front and back parts of the hauling truck, and it is this material that would have lost the most heat.

The total thickness of the overlay, as measured from the cores, was slightly less than 50mm. Permanent deformation wheeltracking tests [BS 96] were conducted on four 200mm diameter cores to determine the rut susceptibility of the mixture. An average rut rate of 1.5mm/h was measured; this is substantially less than the 5mm/h limit set in the specification. It can thus be anticipated that any rutting measured would mainly be due to deformation in the underlying layers. At 20°C the mixture had an Indirect Tensile Stiffness Modulus of 1500MPa (typical 1650MPa @ 4.6% voids, [REA 96]) with a large coefficient of variation (28%) which is most likely due to the variations in void content (29%) [HAR 00]. The S-N curve for the Indirect Tensile Fatigue Test (ITFT) measurements at 20°C are shown in Figure 4. Fatigue parameters and correlations are discussed in more detail later.

Table 2. *Summary of measured properties for asphalt core samples.*

Property	Diameter (mm)	Number of specimens	Mean	Standard deviation	Coefficient of variance
Layer thickness (mm)	100/200	4/12	46.5	3.9	0.08
Void content (%)	100	12	14.1	4.1	0.29
ITSM @ 20°C (MPa)	100	10	1437	398	0.28
*Rut rate @ 60°C(mm/hr)	200	4	1.5	1.0	0.66
* Note : Maximum allowable rate = 5 mm/hr [BS 96]					

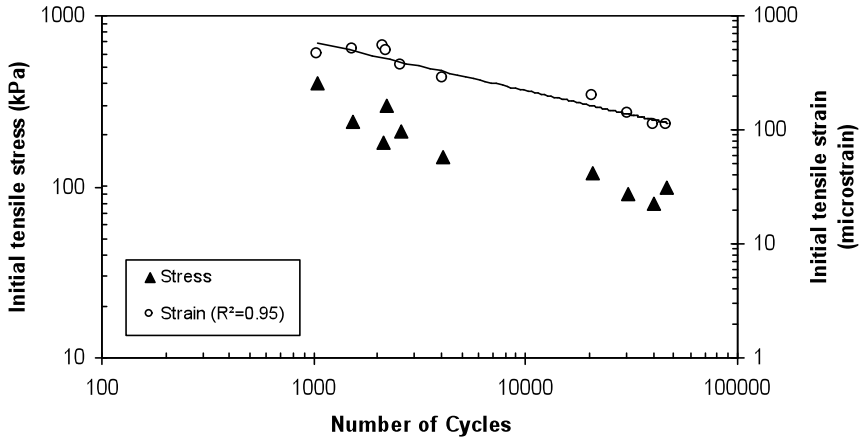

Figure 4. *Indirect Tensile Fatigue Test initial tensile stress and strain data for cored samples.*

3.4. *Crack monitoring*

A similar procedure as described by Miradi et al [MIR 97] was adopted for monitoring the crack growth in the present experimental investigation. Cracks were monitored by tracing any visible cracks in the predetermined monitoring areas on to Perspex sheets (300x300x2mm). The monitoring areas were staggered randomly across the wheelpath and their positions were located with white road marking paint. The pavement surface was investigated prior to testing and all construction defects

were marked accordingly on the Perspex sheets. Subsequent damage was marked in different colours on the same Perspex sheets.

The crack patterns on the sheets were digitised in the laboratory using an Olympus C-840L digital camera under controlled lighting conditions. A schematic illustration of the image capture arrangement is shown in Figure 5. Selection of the monitoring area, filtering of the background and storage of the image data in a compressed, greyscale format (.JPG) were done with the Ulead PhotoImpact image processing package [ULE 96].

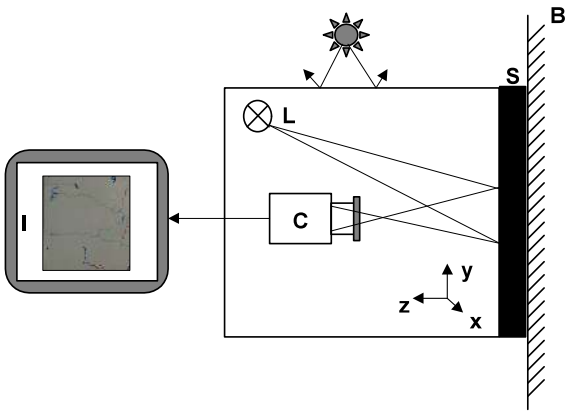

Figure 5. *Schematic of arrangement for digital photography: S = marked perspex sheet; B = white background; C = camera with frame grabber; L = light source; I = image processing.*

The greyscale images were imported into UTHSCSA Image Tool [UTH 96] for image processing and analysis. The dimensions of the monitoring area (300x300mm) were calibrated against the pixel size so that direct dimensional measurements could be established for the digital images. The grey scale images were converted into binary format (consisting of only pure white and pure black pixels) by applying a threshold value. The selection of this threshold value was achieved by applying a range of thresholds and manually selecting the particular value that best represented the crack damage. This same threshold was then applied to all subsequent images.

To calculate the total length of cracks, an algorithm that counts the number of black pixels was applied to the images that were captured with the digital camera. No distinction was made between narrow and wide cracks and all visible defects were recorded with a marker of standard width. Thus, by normalising the area

against the width of the tracing marker, the actual total crack length was determined. The spatial calibration of this data allowed the area to be given in m^2.

Measurements of crack direction were also made on the traced crack network patterns. An image analysis subroutine was used to identify cracks as objects. The major axis angle, i.e., the angle of the longest line drawn through the object to the horizontal, was determined for each object. The major axis angle, normalised to the length of each crack, represents the effective growth direction of each crack.

3.5. *Permanent deformation monitoring*

Permanent deformation was monitored with an optical level at four cross section positions. At each cross section position 14 measurements were taken at 230mm intervals. The exact positions were marked with road marking paint on the pavement surface. A specially constructed attachment was fixed to the end of the levelling staff to ensure that measurements were taken consistently at the same position.

4. Experimental truck specifications

The test section was loaded using a three axle (single front and dual in tandem rear) fixed-bed timber transportation truck. The vehicle had a 10-spring flat-leaf suspension and was fitted with 10R20 tyres. This truck configuration is representative of the heavier carriage used by the timber industry in Ireland. The truck was loaded with timber that gave maximum axle loads of 63kN (front) and 89 and 88kN for the rear tandem axles respectively. The load sharing coefficient (ratio of the load on the heaviest axle to the average load) of the tandem axle was approximately unity, which indicates that a near perfect load distribution was achieved with this configuration.

Tyre contact areas were measured using a hydraulic jack to lift the respective axles off the ground and then lower them onto firm, smooth paper. The imprints were then enhanced using black ink, digitised and effective contact areas (tread area only) determined by using the same image analysis procedure discussed earlier. The measured contact areas and contact pressures used during the loading of the test pavement are listed in Table 3.

5. Data collection routine

The measurement system is shown schematically in Figure 6. The resistive bridges of the strain and pressure transducers were excited and their output voltages

recorded as differential voltages using a Campbell Scientific CR23X micrologger. A laptop microcomputer was used to monitor signal inputs to the datalogger, control all data collection and to retrieve data for subsequent analysis.

Table 3. *Measured contact areas and contact stresses for fully laden truck.*

Axle	Wheel configuration	* Load on wheel assembly (kN)	Effective contact area (m^2)	Nominal tyre-pavement contact stress (kPa)
Front	Single	31.7	0.044	720
Middle	Dual	44.6	0.063	708
Rear	Dual	44.1	0.063	700
* Note: Tyre pressure at 770 kPa				

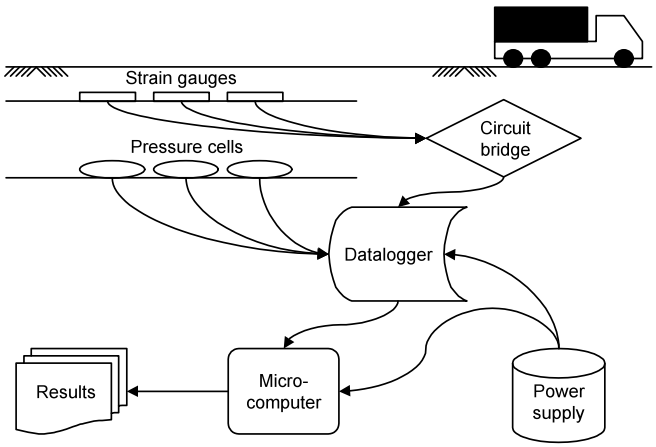

Figure 6. *Measurement arrangement.*

A series of truck traversals was conducted over the test pit so that the initial response of the pavement could be determined from the measurements taken from the strain gauges and pressure cells. The truck was driven at a constant speed of approximately 2 km/h to minimise the effect of road surface roughness. During these initial trials the outer steering wheel was aligned so that it would roll directly over the Group 1 set of sensors (c.f. Figure 2).

After collecting this initial stress-strain data, the experimental section was tracked repeatedly until a network of fatigue cracks was observed on the pavement

surface. Permanent deformation measurements were conducted at regular intervals. Crack tracing only commenced once a visible amount of cracking was observed in the monitoring areas and was only repeated when incremental crack propagation had been observed.

6. Results of pavement monitoring

6.1. *Dynamic response of pavement*

6.1.1. *Measurements from in-situ transducers*

Figure 7 illustrates the pavement response outputs as recorded by the different groups of transducers during dynamic loading. The position of the transducers relative to the loading wheel influenced the recorded levels of strain although the measured stress on the subgrade remained relatively constant, displaying similar peak values corresponding to the passage of individual wheels.

The Group 1 gauges were situated directly under the front and outer middle and rear wheels and consequently they identified the peak levels of strain as each wheel passed overhead. For Group 2 gauges, the front wheel passed adjacent to the edge of the group resulting in lower strain readings. The gap between the dual wheels (of the middle and rear axle) passed over the Group 2 gauges, resulting in a compressive transverse strain. For Group 3 gauges the front wheel passed to the right of the gauges, which consequently recorded lower longitudinal strains than Group 1 and Group 2 gauges and compressive strain in the transverse direction. The inner middle and rear wheels passed straight over the Group 3 gauges resulting in similar strain levels being sensed as by the Group 1 gauges.

The transverse strain pulse remains tensile for the Group 1 gauges as the wheel load passes over the pavement, while the longitudinal strain changes from compression to tension and back to compression. As reported by Huhtala et al [HUH 90], the transverse strain under the steering wheel was higher than the corresponding strain for the dual wheels in the rear tandem axles. However, the longitudinal strain under the steering wheel was similar to the longitudinal strains excited by the rear duals. The Group 1 gauges also indicate that a degree of permanent deformation is experienced in the transverse direction as evidenced by the non-zero levels of strain after loading. No stress reversal takes place and the gradual dissipation of strain can be ascribed to the viscoelastic behaviour of the bituminous layer. The higher transverse strains would indicate that initial fracture would be due to these strains and that damage would be apparent in the form of longitudinal cracking in the wheelpath.

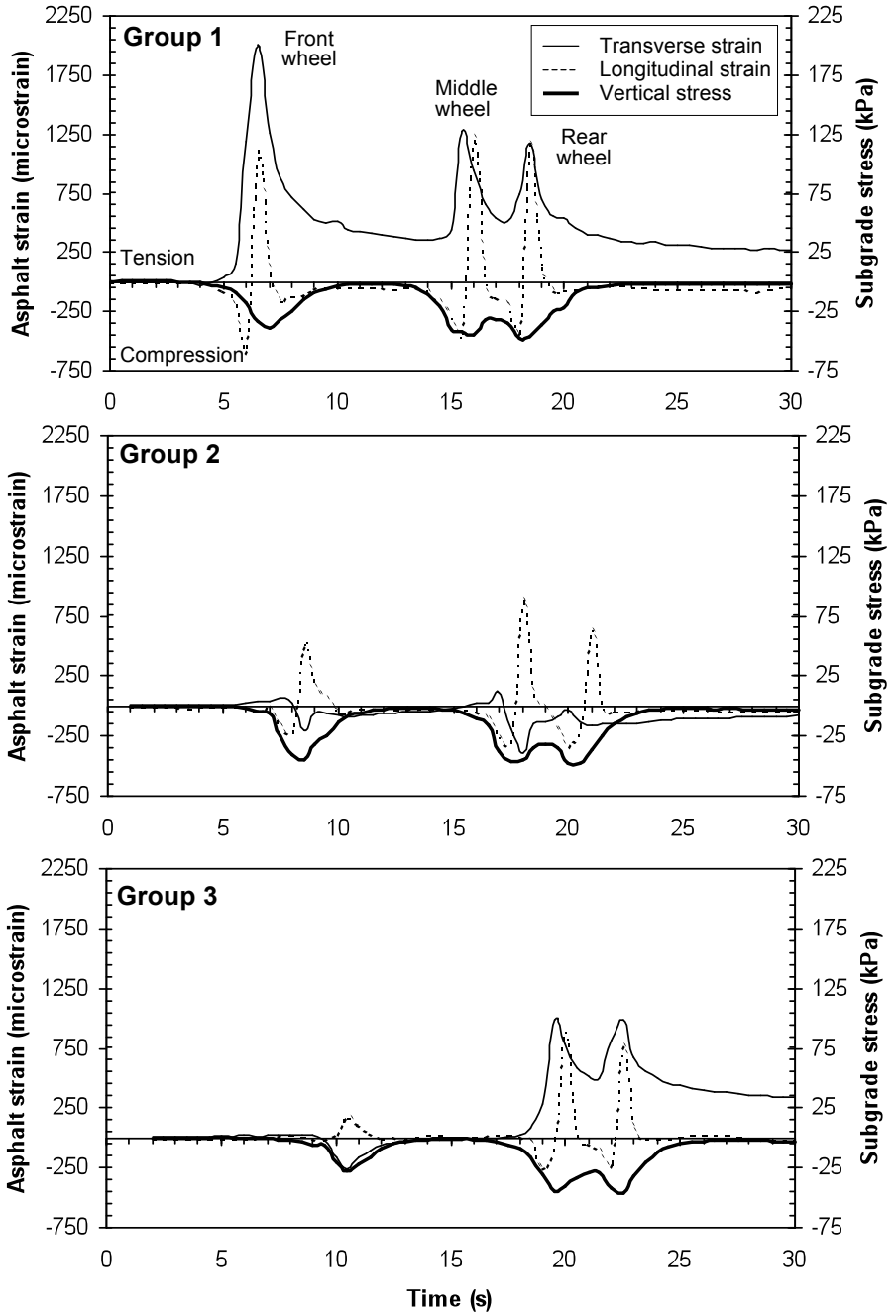

Figure 7. *Typical response sensed from embedded gauges at different positions with reference to loading wheels (vehicle speed = 2km/h). Groups 1, 2 and 3 refer to strain gauge locations identified in Figure 2.*

Examination of the longitudinal strains indicates that the magnitude of the compression pulse preceding the tension pulse was much greater than the compression pulse following the tension pulse. This could be due to the viscoelastic nature of the material masking the second compression pulse because of permanent deformation associated with the tension pulse. An alternative interpretation would be that this is caused by a compression deformation wave travelling ahead of the loading wheel [OWE 01]. A thin stiff layer over a soft elastic subgrade would promote the development of such a deformation wave. The section subjected to compression ahead of the individual wheels extended to a distance of approximately 1m from the centre of the wheels. Gillespie and Karamihas [GIL 94] reported that this distance would be greater with more rigid pavement structures. It was observed that the longitudinal strain dissipated after each wheel load; this would indicate that the pavement responded to the three axles as a series of separate and independent loads in the longitudinal direction. A summary of the measured maximum strains and stresses is given in Table 4. Additional information including the influence of variable tyre pressures and axle loads on this particular pavement structure's response is detailed elsewhere [OWE 01].

Table 4. *Summary of maximum strain and stress measurements.*

Axle	*** Axle load (kN)**	**Strain at bottom of asphalt layer (μstrain)**		**Stress on top of peat subgrade (kPa)**
		Longitudinal	**Transverse**	
Front	63	1097	2000	36.3
Middle	89	1244	1287	39.2
Rear	88	1177	1165	41.1
* Note: Tyre pressure at 770kPa				

6.1.2. *FWD measurements*

To properly evaluate the pavement response the thickness, stiffness and Poisson's ratio of each layer are required. The depth of the pavement structure was determined from the testpit, while Poisson's ratios were assumed for typical materials as identified from the laboratory soil tests [CRO 98, EVD 96]. The pavement structure used in the analysis is listed in Table 5.

Table 5. *General pavement structure of test section (before overlay construction).*

Layer number	Layer	Thickness (mm)	Poisson's ratio
1	Base	200	0.35
2	Subbase	400	0.40
3	Subgrade	-	0.45

The original FWD data set was used with the above pavement structure to determine the depth of the rigid layer with the procedure described by Rohde and Scullion [ROH 90]. The average thickness of the peat above the rigid layer was calculated to be approximately 2m. A second set of FWD deflections was measured after the layer was constructed, and prior to the tracking experiment. A combination of the two deflection sets for the overlaid section is shown in Figure 8. The parameters illustrated include the maximum deflection of the overall pavement structure ($Y_{max} = D_0$, where D_x is the FWD deflection measured at offset x mm from the load centre), the deflection of the upper layers in the pavement or the Surface Curvature Index ($SCI = D_0 - D_{300}$) and the subgrade deflection, ($D_{outer} = D_{1800}$). The second FWD set measured lower deflections in the upper layers, indicating an increase in pavement strength due to the addition of the 50mm overlay. At 17-20m a distinct increase in Y_{max} was identified. This is in the middle of the testpit, as shown in Figure 8. This implies that weakening of the structure occurred in the testpit and consequently that the same in-situ density was not achieved after construction of the pavement layers as had been present prior to construction.

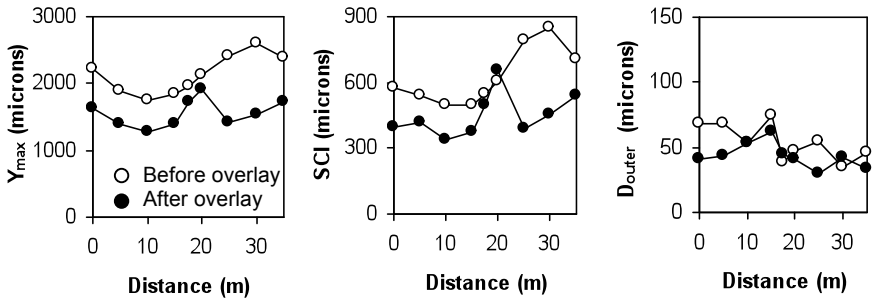

Figure 8. *FWD deflections before and after layer construction.*

In the evaluation of layer moduli, two linear elastic backcalculation programs were used, namely BOWLER [ROH 92] and ELMOD [DYN 99]. Table 6 summarises the representative moduli calculated for the test section using the above mentioned programs. Since the asphalt overlay was less than 50mm thick, the value of its stiffness was fixed and calculated from the measured ITSM (1500MPa @ 20°C) corrected to the pavement temperature at the time of deflection measurement (2300MPa @ 14°C) using a temperature-frequency transformation function for the DBC mixture [HAR 00]. A Poisson's ratio of 0.35 was assumed for the asphalt layer.

A decrease in the backcalculated base modulus was observed, which is possibly due to the stress stiffening characteristics of granular materials [DEB 97]. After the overlay was constructed the base course was subjected to lower stress levels during the deflection measurement that resulted in the lower moduli measured.

Table 6. *Representative backcalculated layer moduli for test section.*

Layer	**Thickness (mm)**	**Backcalculated moduli (MPa)**	
		Before overlay	**After overlay**
Asphalt	50		2300*
Base	200	475	215
Subbase	400	10	20
Subgrade	2000	15	15
* Note: Modulus fixed			

From Figure 8 it was clear that the testpit caused a variation in pavement surface deflection. To compare stresses and strains calculated from the linear elastic pavement model with those measured from the transducers it was decided to use the specific material properties measured from the deflection bowl on top of the testpit. The linear elastic program WESLEA [VAN 89] was used to calculate the stresses and strains at different positions within the pavement structure. The loading configuration of the rear dual and single front axles were used to calculate the strains at the bottom of the asphalt layer and the stress on top of the subgrade. Table 7 summarises the calculated stresses and strains and compares these against the measured values.

The backcalculated moduli lead to the measured stresses and strains being under predicted by a factor of between 2.3 and 4.8. A possible reason for the large

variation in these results is the speed of loading. FWD deflections are measured under a load corresponding to a vehicle speed of 60km/h (±16Hz), while measurements from the pavement transducers were taken at a wheel speed of approximately 2km/h.

Table 7. *Summary of predicted and measured stresses and strains calculated from backcalculated moduli for the testpit deflection bowl.*

Parameter	Measured	Predicted
Layer Moduli (MPa)		
Asphalt		2300
Base		150
Subbase		20
Subgrade		15
Longitudinal asphalt strain (μstrain)		
Front	1097	416
Rear	1177	402
Transverse asphalt strain (μstrain)		
Front	2000	416
Rear	1165	340
Subgrade stress (kPa)		
Front	36.3	13.7
Rear	41.1	17.9

6.1.3. *Measurement of permanent deformation*

Incremental change in the cross section profile over the length of the monitoring section was insignificant which suggests that failure was mainly a fatigue phenomenon. Towards the end of the test a small amount of permanent deformation (< 10mm) was observed in the outer wheel track.

6.1.4. *Crack monitoring*

The first cracks were visible on the surface after approximately 2000 experimental truck loadings. The cracks appeared close to the Group 1 gauges and were aligned in the longitudinal direction. This confirmed the assumption that transverse strains were responsible for crack initiation.

Figure 9 shows the increase of crack length within the wheelpath with the number of experimental truck passes. The increase of crack length follows an almost sigmoidal pattern with an initial rapid increase being followed by a slower increase.

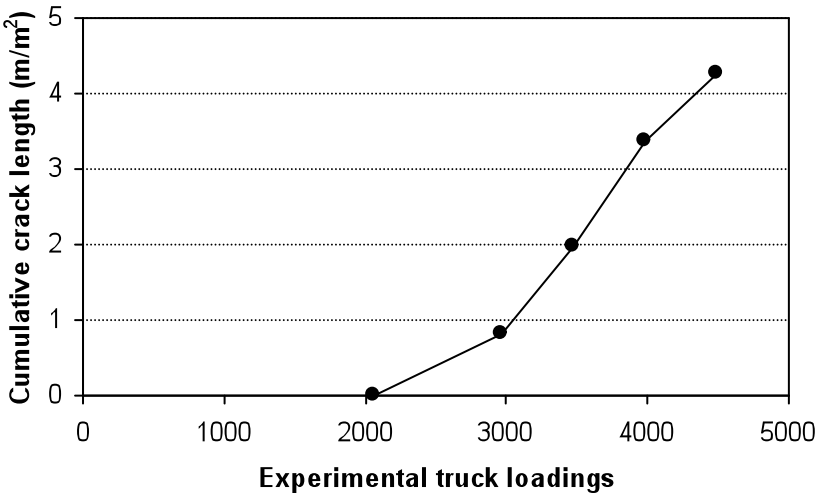

Figure 9. *Variation of cumulative crack length with truck loading cycles.*

Figure 10 describes a typical example of traced cracks after the first and final tracings. On average, the crack angle changed from 31° to 41°, from the plane parallel to the direction of travel. Therefore, the majority of cracks formed in the longitudinal direction ($C_D^{eff} < 45°$). This observation suggests that cracks mainly initiate in the longitudinal direction with subsequent lateral networking. This implies that while the transverse strain governs the initiation of fatigue cracks, the subsequent networking of the cracks is influenced by longitudinal strains. The final crack pattern on the surface was typical of crocodile cracks as shown in Figure 11.

6.2. *Predicted and observed fatigue damage*

The total number of experimental truck passes required to cause visual evidence of crack initiation was approximately 2000 cycles. The pavement temperature during the tracking experiment was not constant but varied about an average of 6°C (±4°C). As discussed earlier, the transverse tensile strain at the bottom of the asphalt layer was responsible for causing the first longitudinal cracks to appear. Values for the initial transverse tensile strain in the DBC layer was calculated using the linear elastic pavement model and the in situ H-gauge measurements. A temperature correction to 6°C was applied to the strain values based on the initial asphalt stiffness.

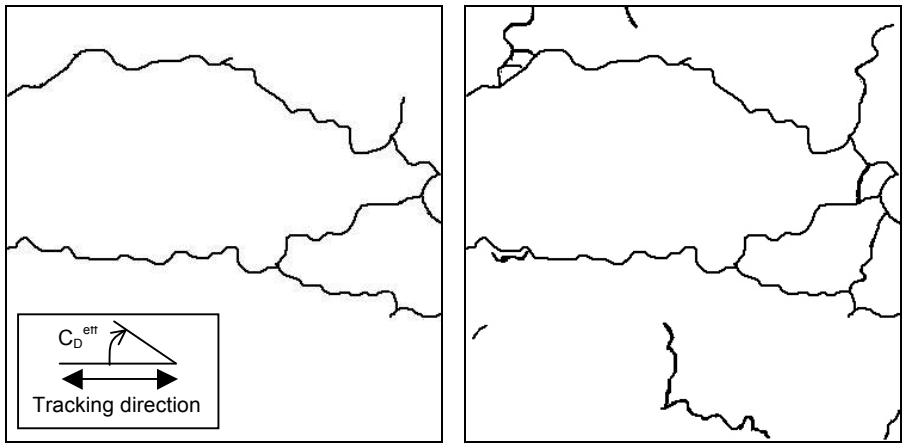

Figure 10. *Change in crack direction over fatigue life.*

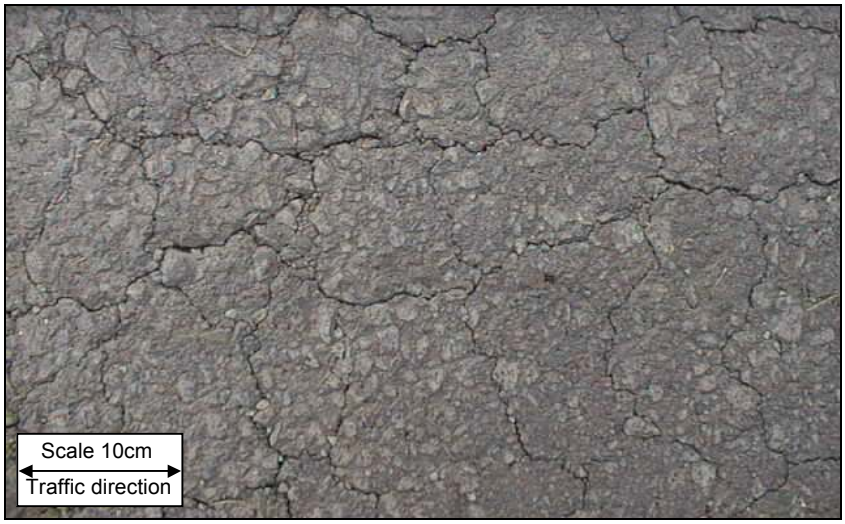

Figure 11. *Final crocodile crack pattern observed at 'failure' of road section.*

The fatigue relationship for the DBC mixture was determined from the ITFT results (shown in Figure 4), which consequently lead to the following expression for the number of cycles to crack initiation, *N*:

$$N = 3.3068 \times 10^{9} \varepsilon^{-2.3546} \quad (1)$$

where ε has units of μstrain. Equation (1) was subsequently used to predict the number of axle loadings to crack initiation for both the front and rear dual axles. The equivalent truck passes was determined using Miner's law applying a split of 1/3 front axle and 2/3 rear axle loadings. The predicted fatigue lives are summarised in Table 8, in terms of axle and truck loadings.

Table 8. *Predicted number of fatigue cycles to crack initiation.*

Method	Axle	Initial transverse tensile strain (microstrains)	Predicted axle cycles to crack initiation (Eq. 1)	Equivalent truck passes
Measured from in-situ gauges	Front	1720	80	153
	Rear	1002	284	
Calculated from FWD deflections	Front	416	2252	2374
	Rear	402	2441	
Note: 2060 actual truck passes were applied to cause crack initiation.				

The calculated fatigue life based on the in-situ measured strain under predicted the measured fatigue life (2060 cycles) by a factor of 13.5, while the fatigue life based on the calculated strain slightly over predicted the measured fatigue life. Although it can be argued that the strain gauges over predict the strain levels, the factor of 13.5 may be considered appropriate since the effects of healing and traffic wander were ignored. During the experiment, loading was not applied at night, during weekends and because of maintenance. Groenendijk et al [GRO 97] used a factor of 4 for healing during testing on the LINTRACK facility in Delft (The Netherlands). During tracking the experimental truck was allowed to randomly wander in the wheelpaths, and this naturally resulted in less loading being applied to a specific point in the pavement. Traffic wander factors of 1.0 to 2.5 have been reported [VER 74]. The ITFT test is said to determine asphalt fatigue life to crack initiation regardless of the asphalt layer thickness. The standard specimens tested were 40mm in thickness although the pavement thickness was closer to 50mm. It is anticipated that a thicker structure would require more loading cycles to accumulate and propagate damage through its full depth.

7. Conclusion

An accelerated loading test was performed on a 50mm DBC macadam layer overlaying a granular base and subbase on a weak peat subgrade. The test road was continuously tracked with a fully laden three axle timber haulage truck until a network of fatigue cracks was observed on the pavement surface. The response of the layer was monitored using in-situ gauges, FWD deflections and visual inspections of crack and rut formation. Pavement healing and limited traffic wander occurred during the test sequence.

It was found that the transverse horizontal tensile strain is the most critical parameter with respect to crack initiation. This was confirmed by the predominant appearance of longitudinal cracks in the wheelpath. The single front steering wheel induced higher transverse strains than the tandem duals, indicating that this axle configuration is critical in initiating asphalt fatigue damage. Transverse strain pulses showed a level of residual strain, the magnitude of which varied with lateral position on the wheel track.

Calculated stresses and strains from the linear elastic model were lower than the predicted values measured from the in-situ transducers, particularly the transverse strain caused by the single front steering wheel and the vertical stress on the subgrade. The main failure mode for the test section was fatigue cracking in the wheelpath which was accompanied by a small amount of rutting (< 10mm). Surface visible cracks initiated mainly in a longitudinal direction but with increasing experimental truck cycles, more transverse cracking was observed.

Predicted fatigue life to crack initiation, using the ITFT S-N relationship and the in-situ measured strain levels, *underestimated* the performance of the test section. Factors that were not accounted for in the prediction, such as material healing, traffic wander and fatigue specimen size, would possibly lead to longer fatigue estimates.

8. Acknowledgements

The authors would like to express their gratitude to the following organisations for their support and assistance: Enterprise Ireland (Applied Research Grants HE/1996/148 and HE/1998/288), Irish Forestry Board, National Council for Forest Research and Development (COFORD), National Roads Authority, Roadstone Dublin and Wicklow County Council.

9. References

[BS 93] BS 4987: PART 1, 'Coated Macadams for roads and other paved areas.' British Standards Institution, London, England, 1993.

[BS 96] BS 598: PART 110, 'Sampling and examination of bituminous mixtures for roads and other paved areas: Part 110. Method of test for the determination of the wheel-tracking rate.' British Standards Institution, London, England, 1996.

[CRO 98] CROW, 'Deflection profile - not a pitfall anymore: survey and interpretation methodology falling weight deflection measurements.' CROW Record 17, Information and technology Centre for Transport and Infrastructure, Netherlands, 1998.

[DAV 96] DAVITT, S.; KILLEEN, R.C., 'Maintenance techniques for bog roads.' NRA Report RC.375, National Roads Authority, Ireland, 1996.

[DEB 97] DE BEER, M.; VAN DER MERWE, C.J.; ROHDE, G.T., 'Rehabilitation design of flexible pavements in South Africa.' Research Report 93/296, Department of Transport, South Africa, 1997.

[DYN 99] DYNATEST, 'ELMOD 4.4 version 1.2.2.' Dynatest International Consulting Ltd., Denmark, 1999.

[EVD 96] EVDORIDES, H.T.; SNAITH, M.S., 'A knowledge based analysis process for road pavement condition assessment.' Proceedings of the Institute of Civil Engineers, Vol. 117 no. 3, pp. 202-210, 1996.

[GIL 94] GILLESPIE, T.D.; KARAMIHAS, S.M., 'Heavy truck properties significant to pavement damage.' Vehicle-Road Interaction, ASTM STP 1225, edited by B.T. Kulakowski, Philadelphia, USA, pp. 52-63, 1994.

[GRO 97] GROENENDIJK, J., VOGELSANG, C.H.; MIRADI, A.; MOLENAAR, A.A.A., 'Linear tracking performance tests on full-depth asphalt pavement.' Transportation Research Record 1570, Transportation Research Board, Washington, USA, pp. 39-47, 1997.

[HAR 00] HARTMAN, A.M., 'An experimental investigation into the mechanical performance and structural integrity of bituminous pavement mixtures under the action of fatigue load conditions.' PhD Thesis, University College Dublin, Ireland, 2000.

[HAR 01a] HARTMAN, A.M., GILCHRIST, M.D., WALSH, G., 'Effect of mixture compaction on indirect tensile stiffness and fatigue.' ASCE Journal of Transportation Engineering, Vol. 127 no. 5, 2001 (in press).

[HAR 01b] HARTMAN, A.M., GILCHRIST, M.D., NOLAN, D, 'Wheeltracking fatigue simulation of bituminous mixtures.' International Journal of Road Materials and Pavement Design, 2001 (in press).

[HUH 90] HUHTALA, M.; ALKIO, R.; PIHIJAMAKI, J.; PIENIMAKI, M.; HALONEN, P., 'Behaviour of bituminous materials under moving wheel loads.' Proceedings of the Association of Asphalt Paving Technologists, Vol. 59, pp. 422-442, 1990.

[MIR 97] MIRADI, A.; GROENENDIJK, J.; DOHMEN, L.J.M., 'Crack development in linear tracking test pavements from visual survey to pixel analysis.' Transportation Research Record 1570, Transportation Research Board, Washington, USA, pp. 48-54, 1997.

[OWE 01] OWENDE, P.; HARTMAN, A.M., WARD, S.M.; GILCHRIST, M.D.; O'MAHONY, M.J., 'Minimising distress on flexible pavements using variable tire pressure.' ASCE Journal of Transportation Engineering, Vol. 127 no. 3, pp. 254-262, 2001.

[O'MA 00] O'MAHONY, M.J.; VEBERSCHAER, A.; OWENDE, P.; WARD, S.M., 'Bearing capacity of forest access roads built on peat soils.' Journal of Terramechanics, Vol. 37 no. 3, pp. 127-138, 2000.

[REA 96] READ, J.M., 'Fatigue cracking of bituminous paving mixtures.' PhD Thesis, University of Nottingham, England, 1996.

[ROH 90] ROHDE, G.T.; SCULLION, T., 1990, 'Modulus 4.0: Expansion and validation of the MODULUS backcalculation system.' Research Report No. 1123-3, Texas Transportation Institute, Texas A & M University, Texas, USA.

[ROH 92] ROHDE, G.T., 'BOWLER version 2.0.' BIS Ltd., Pretoria, South Africa, 1992.

[TAB 89] TABATABAEE, N.; SEBAALY, P.; SCULLION, T., 'Instrumentation for flexible pavements.' FHWA Report RD-89-084, Washington USA, 1989.

[ULE 96] ULEAD SYSTEMS, 'Ulead PhotoImpact Version 3.0SE.' Ulead Systems International Inc., Taipei, Taiwan, 1996.

[ULL 87] ULLIDITZ, P.P., 'Pavement analysis.' Pub. Elsevier Science, Netherlands, 1987.

[UTH 96] UTHSCSA IMAGE TOOL, 'Image Tool Version 2.0.' University of Texas Heath Science Centre Department of Dental Diagnostic Science, San Antonio, Texas, USA, 1996.

[VAN 89] VAN CAUWELAERT, F.J.; ALEXANDER, D.R.; WHITE, T.D.; BARKER, W.R., 'Multilayer elastic program for backcalculating layer moduli in pavement evaluation.' Non Destructive Testing of Pavements and Backcalculation of Moduli, ASTM STP 1026, Philadelphia, USA, pp. 171-188, 1989.

[VER 74] VERSTRAETEN, J., 'Loi de fatigue en flaxion répétée des mélanges bitumineux.' Bulletin de Liaison des Laboratoires des Ponts et Chaussees n º70, Paris, France, 1974.